High-Resolution ZTE Imaging of Human Teeth

M. Weiger[1,2], K. P. Pruessmann[3], A-K. Bracher[4], S. Köhler[2], V. Lehmann[5], U. Wolfram[6], and V. Rasche[4]

[1]Bruker BioSpin AG, Faellanden, Switzerland, [2]Bruker BioSpin MRI GmbH, Ettlingen, Germany, [3]Institute for Biomedical Engineering, University and ETH Zurich, Zurich, Switzerland, [4]Internal Medicine II, University of Ulm, Ulm, Germany, [5]Bruker BioSpin GmbH, Rheinstetten, Germany, [6]Institute of Orthopaedic Research and Biomechanics, University of Ulm, Ulm, Germany

Introduction Imaging of the mineralised layers of teeth (dentin and enamel) is the basis for the diagnosis of demineralisation and caries lesions. The current clinical standard comprises x-ray imaging methods. However, besides the application of ionising radiation, these methods are known to show only moderate sensitivity for early demineralisations, to underestimate caries lesions, and to be limited in the identification of secondary lesions. Also, MRI has been proven capable of visualising the mineralised layers of teeth [1-4] as well as caries lesions [5, 6]. In particular, for the identification of early lesions and the real extent of caries lesions, superior sensitivity of MRI compared with x-ray-based methods has been demonstrated [6]. Due to the short transverse relaxation times of dentin and enamel on the order of a few hundreds of milliseconds [7, 8], efficient dental imaging is preferably performed with methods using 3D radial centre-out *k*-space encoding. Particularly, the UTE (ultra-short echo time) technique [9, 10] and SWIFT, using frequency-swept excitation with simultaneous acquisition [11], have been employed for this purpose. In the present work, the short-T_2 capabilities, robustness, and efficiency of zero echo time (ZTE) MRI was used for high-resolution in-vitro imaging of human teeth and compared with UTE as well as micro computed tomography (µCT).

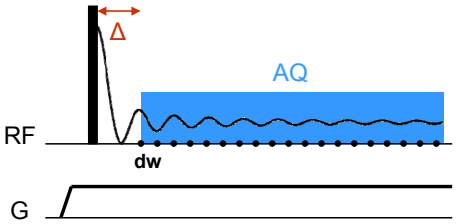

Figure 1 *ZTE acquisition scheme with dwell time* dw *and dead time* Δ.

Methods and Materials In ZTE imaging (Fig. 1), zero echo time is achieved by switching on the readout gradient before RF excitation with a high-bandwidth hard pulse [12, 13] (Fig. 1). The data obtained in this way is incomplete in the *k*-space centre due to the initial dead time Δ associated with RF pulse duration, transmit-receive (T/R) switching, and digital filter build-up. This situation is addressed by radial acquisition oversampling and algebraic reconstruction, involving finite support extrapolation [14, 15]. ZTE protocols were designed with the following range of imaging parameters: matrix size $(96\text{-}160)^3$, resolution $(312\times188^2$ - $144\times113^2)$ µm^3, flip angle 3°, TR 1-2 ms, 29130-80892 radial readouts, 1-32 averages, and scan time 29 sec - 27 min. For the acquisition bandwidth of 200 kHz, the sequence timing was: dwell time dw = 5 µs, readout duration 240-400 µs, oversampling 4, T/R switching duration 4.5 µs, RF pulse duration 1 µs, resulting in the dead time Δ = 1.375 dw. UTE was performed with the same parameters as ZTE, yet with a gradient ramp of 190 µs, which started 10 µs after the RF pulse. *K*-space trajectories and zero-order phase errors were measured and taken into account during image reconstruction. All MRI data were acquired on a µMRI-system (Bruker 11.7 T vertical wide-bore magnet, AVIII console, Micro2.5 probe head, gradient system with maximum strength 150 G/cm, and RF resonators with 10 or 15 mm diameter). The µCT data was acquired at 70 kV and 141 µA with a spatial resolution of (15 µm)³ (Skyscan 1172, Kontich, Belgium). Projection images were obtained using φ = 180° rotation with dφ = 0.7° and an exposure time of 316 ms. Smoothing with an asymmetric boxcar filter of size 1 as well as ring-artifact and beam-hardening corrections were applied. Imaging was performed on twelve extracted human teeth (incisors and molars) with various defects and treatment which were stored in water to prevent drying. Manual rigid-body registration was performed between the different data sets. Statistical relevance was tested applying a two-tailed paired Student's t-test.

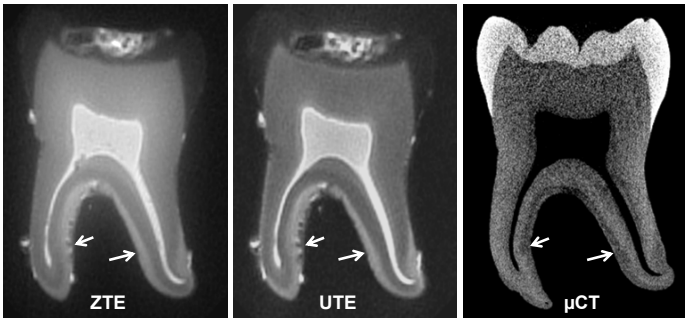

Figure 2 *Comparison of ZTE, UTE, and µCT of an extracted human molar.*

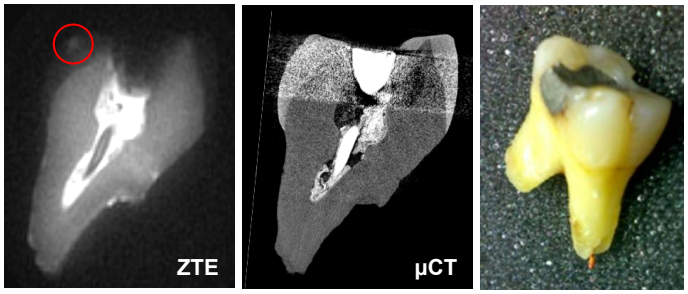

Figure 3 *Caries lesion detected in ZTE (red circle) but not in µCT due to streaking artefacts caused by an amalgam filling.*

Results Figure 2 shows images of a molar obtained with the different techniques. With ZTE, dentin and enamel are clearly delineated. The blurred high signal observed on the masticatory surface probably originates from water embedded in the fissures seen with µCT. The prominent signal variations within the dentin (arrows) correspond to only a slight contrast in µCT. The UTE images appear very similar as ZTE but exhibit some reduction in signal intensity for both materials. This observation is supported by the analysis of SNR and CNR (Fig. 4), showing significant signal differences between the two mineral layers and the background. In ZTE, SNR as well as CNR are significantly ($p<0.05$) larger than in UTE. Figure 3 compares ZTE and µCT in the presence of an amalgam filling. Despite state-of-the-art processing in µCT, the streaking artefacts due to long-range beam hardening considerably affect the image quality. In ZTE, the susceptibility-related blurring is only moderate, owing to the high acquisition bandwidth. Consequently, the slight caries lesion is only detected in MRI.

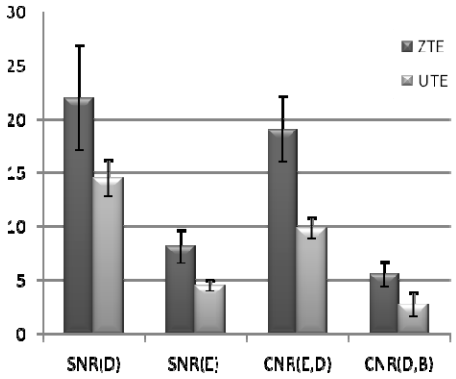

Figure 4 *Analysis of signal-to-noise-ratio (SNR) and contrast-to-noise-ratio (CNR) in ZTE and UTE. D = dentin, E = enamel, B = noise background.*

Conclusion ZTE has been demonstrated to provide excellent image quality for in-vitro dental MRI. Compared with UTE, superior SNR and CNR were found and attributed to reduced T_2-weighting and immediate, full-bandwidth encoding. For both MRI techniques, better sensitivity to demineralisation was observed compared with the x-ray counterpart. Similar to UTE [6, 10], in-vivo application of ZTE is a promising perspective but requires dedicated RF hardware for rapid T/R switching.

References [1] Baumann MA, Oral Surg Oral Med Oral Pathol 75 (1993) 517 [2] Wu Y, PNAS 96 (1999) 1574 [3] Appel TR, Oral Surg Oral Med Oral Pathol Oral Radiol Endod 94 (2002) 256 [4] Gruwel M, Appl Phys A 88 (2007) 763 [5] Lloyd CH, Caries Res 34 (2000) 53 [6] Bracher A, ISMRM (2010) 2974 [7] Schreiner LJ, Biophys J 59 (1991) 629 [8] Funduk N, MRM 1 (1984) 66 [9] Glover G, JMRI 2 (1992) 47 [10] Boujraf S, ISMRM (2009) 4518 [11] Idiyatullin D, ISMRM (2010) 543 [12] Hafner S, MRI 12 (1994) 1047 [13] Weiger M, ISMRM (2010) 695 [14] Jackson J, MRM 11 (1989) 248 [15] Kuethe DO, JMR 139 (1999) 18